PLANETARY SCIENCE

Imaging deep-mantle plumbing beneath La Réunion and Comores hot spots: Vertical plume conduits and horizontal ponding zones

Mathurin Dongmo Wamba[1]*, Jean-Paul Montagner[2], Barbara Romanowicz[2,3,4]

Whether the two large low–shear velocity provinces (LLSVPs) at the base of Earth's mantle are wide compact structures extending thousands of kilometers upward or bundles of distinct mantle plumes is the subject of debate. Full waveform shear wave tomography of the deep mantle beneath the Indian Ocean highlights the presence of several separate broad low-velocity conduits anchored at the core-mantle boundary in the eastern part of the African LLSVP, most clearly beneath La Réunion and Comores hot spots. The deep plumbing system beneath these hot spots may also include alternating vertical conduits and horizontal ponding zones, from 1000-km depth to the top of the asthenosphere, reminiscent of dyke and sills in crustal volcanic systems, albeit at a whole-mantle scale.

INTRODUCTION

Whether hot spot volcanism is due to "plumes" of hot material anchored in the mid or deep mantle (*1*) or is an expression of shallow upper-mantle processes (*2*) has been the subject of continued debate in the geophysical community. Mantle plumes may also be at the origin of flood basalt eruptions (*3*) and are thought to have played a major role in continental breakup (*1*). Global seismic tomography has provided evidence for the presence of broad plume-like conduits rooted at the core-mantle boundary (CMB) within the two large low–shear velocity provinces (LLSVPs) beneath the Pacific and Africa (*4*) and extending through the mantle in the vicinity of major hot spots (*5*). One of the major hot spot volcanoes located close to the African LLSVP is La Réunion hot spot, which is thought to be the surface expression of a mantle plume that led to one of the major volcanic cataclysms and the setting up of the Deccan Traps, ~65 million years ago (*6*). Among Indian Ocean hot spots, La Réunion has the largest buoyancy flux (1.9 Mgs^{-1}) (*7*) and exhibits the highest $^{3}He/^{4}He$ ratio (*8*, *9*), suggesting that it may be a primary plume originating deep in the lowermost mantle according to the classification of (*10*). Other Indian Ocean hot spots (Marion, Kerguelen, Comoros, and Crozet) have a lower buoyancy flux (<1.0 Mgs^{-1}) (*7*), which may indicate an origin in a different, shallower, boundary layer or a different stage in the life of a plume. The morphology of La Réunion plume, its relation to other plumes beneath Africa and the Indian Ocean, and the depth of their respective roots remain unclear. A recent study (focused beneath the Indo-African plate, excluding the Southern-East of the Indian Ocean) based on seismic travel time tomography has proposed that the African LLSVP consists of a wide continuous trunk extending from the CMB to ~1500-km depth, from which several branches with complex shapes extend upward toward hot spots, among them is La Réunion (*11*). On the other hand, the broad continuous nature of the LLSVPs has been questioned, arguing, in contrast, that they are formed of a bundle of distinct mantle plumes that extend as separate columns across the mantle from a relatively thin (<200-km-tall) low-velocity and possibly denser base (*12*). To examine these questions further, we have performed regional full waveform inversion (FWI) of three-component teleseismic records containing both surface waves and body waves, illuminating mantle shear velocity structure beneath the Indian Ocean (see details in methods in section S1). The first tomographic models of this region used data from only sparsely spaced land stations and were limited to the uppermost 400 km of the mantle, with a lateral resolution of ~1000 km (*13*, *14*). The expansion of broadband networks around the Indian Ocean in the past few decades, as well as the recent deployment of an array of broadband ocean bottom seismometers around La Réunion hot spot Réunion Hotspot and Upper Mantle -Réunions Unterer Mantel [RHUM-RUM (*15*)], and the temporary experiments Madagascar-Comoros-Mozambique and Seismological Signatures in the Lithosphere/Asthenosphere system of Southern Madagascar [MACOMO (*16*) and SELASOMA (*17*)] around Madagascar, Mascareignes islands, and southeast Africa have made it possible to better constrain the anisotropic structure in the upper mantle using long-period surface waves (*18*) and SKS splitting measurements (*19*). In a recent study, we applied FWI to fundamental mode and overtone three-component surface wave data to further constrain radially anisotropic structure from the upper mantle down to ~1000-km depth (*20*). Here, we extend the latter study to the rest of the lower mantle by including teleseismic body waveforms down to a 30-s period. Fixing the upper part of the model down to ~800-km depth to that of model SEMINDO (*20*), we consider the global model SEMUCB-WM1 (*5*) as a starting model below that depth and invert teleseismic waveforms that contain body phases that sample the deep mantle beneath the Indian Ocean, such as S, converted P to S and S to P, as well as ScS and ScSn, up to distances of ~90° and perform three iterations of FWI to obtain a higher-resolution image of the lower mantle (for methodology, see section S1).

[1]Department of Geosciences, Guyot Hall, Princeton University, Princeton, NJ 08544, USA. [2]Université de Paris/Institut de Physique du Globe de Paris, UMR CNRS 7154, Paris, France. [3]Collège de France, 11 Place Marcelin Berthelot, 75005 Paris, France. [4]Berkeley Seismological Laboratory, 291 McCone Hall, Berkeley, CA 94720, USA.
*Corresponding author. Email: mw1685@princeton.edu

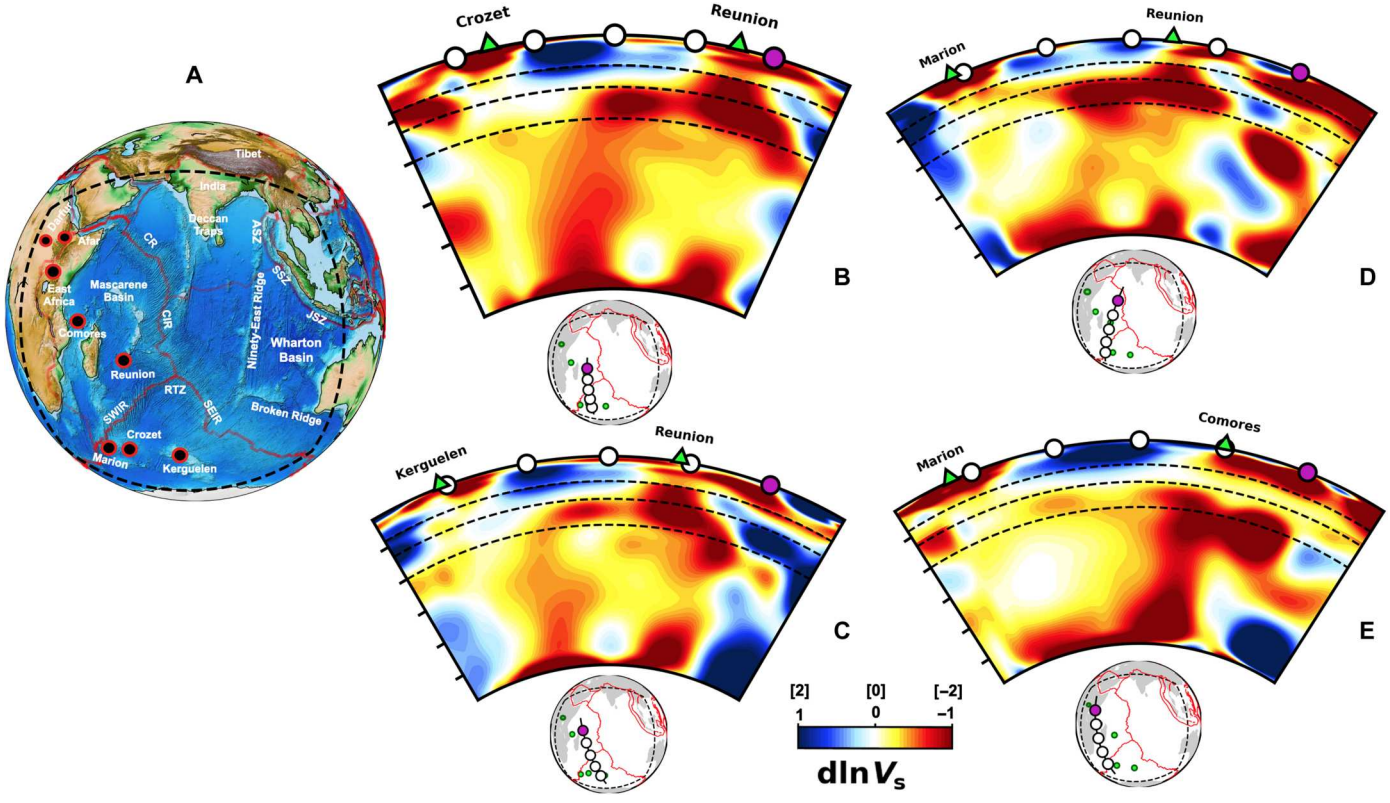

Fig. 1. 2D depth cross sections in model SEMINDO-WM3 in the vicinity of several hot spots in the Indian Ocean. (**A**) Geological map of the region under study, highlighting hot spots (dark circles) and salient geological features: Carlsberg Ridge (CR), Central Indian Ridge (CIR), Southwest Indian Ridge (SWIR), Southeast Indian Ridge (SEIR), Rodrigues Triple Junction (RTZ), Andaman subduction zone (ASZ), Sumatra subduction zone (SSZ), and Java subduction zone (JSZ). The FWI domain is indicated by a black dashed line. (**B** to **E**) 2D depth cross sections from the CMB to 60-km depth, displaying relative perturbations in shear velocity (dlnV_s) with respect to the average at each depth, in percent, showing distinct low–shear velocity conduits extending from the CMB to the top of the lower mantle in the vicinity of several hot spots (green triangles). These quasi-vertical conduits merge into a horizontally elongated region in the depth range of ~660 to 1000 km. Another horizontally elongated zone is shown in the asthenosphere in the depth range of ~250 to 100 km (B to E). Small maps beneath each cross section indicate its geographical location. To emphasize lower-mantle features in the cross sections, we use a different saturation of the color scale for the upper mantle (dln V_s ~ −2%) and the lower mantle (dln V_s ~ −1%) as indicated above the color bar. Broken lines in the cross sections indicate depths of 400, 660, and 1000 km, respectively.

RESULTS

Separate plume conduits in the lower mantle

While our model spans the entire Indian Ocean (Fig. 1A), we here focus on the region surrounding La Réunion and Comores hot spots. La Réunion was classified as the surface expression of a primary mantle plume (*10*), and more recently, both hot spots appeared to correspond to resolved lower-mantle plumes (*5*). Specifically, the resulting lower-mantle model (SEMINDO-WM3), combined with SEMINDO (*20*) for the top 800 km, shows at least three separate columns of low-velocity material originating at the CMB and extending vertically across the lower mantle up to around 1000-km depth, as visible in two-dimensional (2D) depth cross sections (Fig. 1, B to E). In the depth range of ~1000 to 660 km, these columns appear to be deflected horizontally over large distances, defining a strong and broad low-velocity body, suggesting the presence of a horizontally elongated ponding zone for the hot plume material. At shallower depths, a more vertically oriented conduit appears to link this low-velocity zone to specific hot spot volcanoes at the surface. In both cases, the quasi-vertical part of the plume in the lower mantle is offset several hundred kilometers away from the surface location of the hot spot (Fig. 1). Conduits beneath Crozet (Fig. 1B), Kerguelen (Fig. 1C), and possibly Marion (Fig. 1, D and E) appear weaker, likely due to poorer resolution at the border of our inversion domain, but the horizontal deflection around 1000-km depth is also observed. The mantle plumes that feed these two hot spots may be closer geographically in the lower mantle than near the surface (for example, Marion and Réunion in Fig. 1D or Réunion and Kerguelen in Fig. 1C). Resolution tests (section S3) rule out the presence of simple conduits extending vertically all the way from the CMB to the corresponding hot spots (figs. S9 to S12). The entire structure of upwellings is 3D and better illustrated in 3D plots (Fig. 2), since several lower-mantle plumes appear to feed the same low–seismic velocity ponding zone (LSVPZ) in the lower-mantle extension of the transition zone in the depth range of 660 to 1000 km (sometimes also referred to as the lower-mantle transition zone). We note that the upper-mantle conduits that originate from the LSVPZ are not necessarily centered in the same vertical plane as their lower-mantle counterparts. This conduit system consists of five stages, which we interpret as representing plume flow across the mantle: quasi-vertical in the lower up to 1000-km depth and upper mantle between ~660- and 250-km depth; quasi-horizontal in the extended

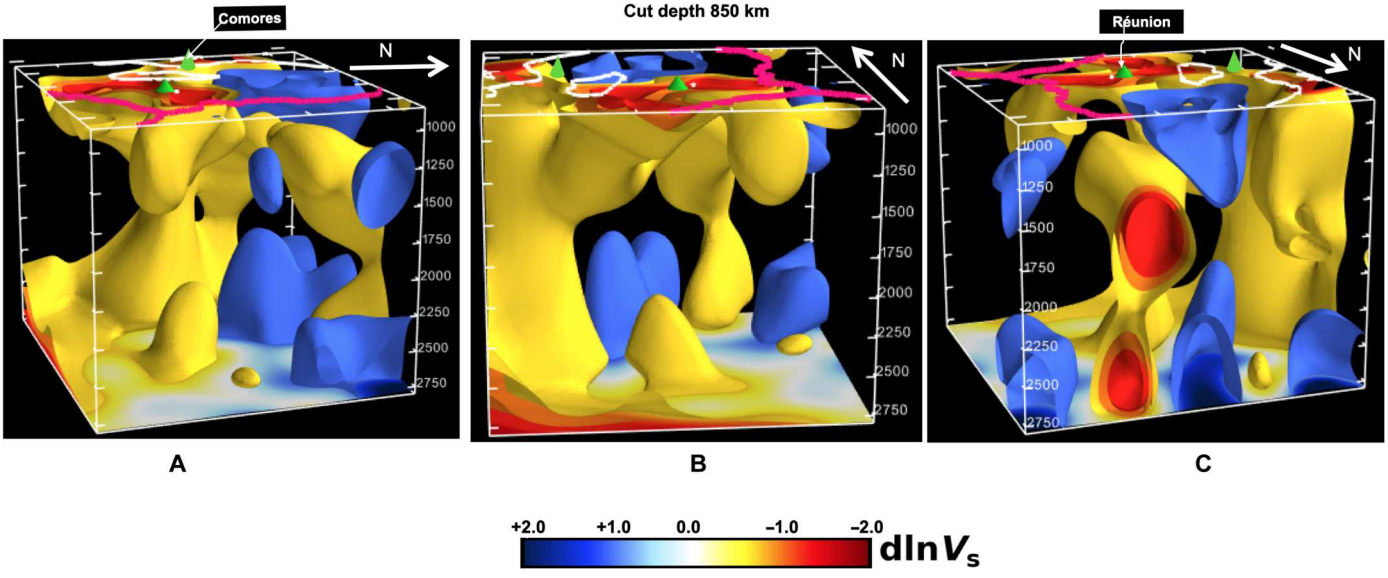

Fig. 2. 3D representation of a subvolume of model SEMINDO-WM3 around La Réunion hot spot, from the CMB to 850-km depth. The model is shown looking from the East (**A**), the South (**B**), and the North (**C**). Yellow and light blue colors indicate the contours of relative velocity perturbations ($d\ln V_s = dV_s/V_s$) at −1% and +1%, respectively. Different views highlight the presence of three separate low-velocity conduits in the lower mantle. In (A) and (B), we note the presence of a low-velocity feature rooted at the CMB, which extends only ~600 km into the mantle. This may represent the "birth" of a plume or the partial expression of the broad base of a poorly resolved thinner plume. The top surface of the volume shown cuts through the horizontally spreading low-velocity channel beneath the Comores and La Réunion located in the depth range of 660 to 1000 km. Land outlines (e.g., Madagascar) are projected on this surface as white lines, and red lines indicate the Indian mid-ocean ridges. Hot spot (Comores and Réunion) locations are projected as green cones. White arrow points to the North. The depth scale is shown on the side of each subvolume. The blue anomalies correspond to regions of faster than average velocities, associated with subducted slabs or their remnants.

transition zone (1000- to 660-km depth) and in the asthenosphere (~250- to ~100-km depth), e.g., Fig. 1 (B to D); and quasi-vertical again toward the surface. It forms a complex 3D structure, making it difficult to directly connect a particular lower-mantle plume to its surface expression in a hot spot volcano. We propose that the horizontally oriented pool of low seismic velocities (LSVPZ) likely represents a decoupling shear zone (*21*) fed from below by hot material ascending in broad, distinct, lower-mantle plumes rooted at the CMB. This material, which may spread horizontally through pressure-driven flow, then serves as secondary source for upper-mantle plumes that feed several Indian Ocean hot spots.

Relation between La Réunion plume and the Central Indian Ridge

Above the zone of horizontal spreading in the extended transition zone, a vertically oriented conduit is present almost directly beneath La Réunion hot spot (Fig. 1, B to D), rooted in the LSVPZ and extending from ~660 km to asthenospheric depths (*20*). This is seen in the 3D rendering of model SEMINDO-WM3 in Fig. 3, in which the upper surface is cut at successively shallower depths (e.g., 200, 300, and 400 km) in the upper mantle. Around 200-km depth, another horizontally elongated zone of lower than average shear velocity extends, on the one hand, west toward the Mascareignes Basin Asthenospheric reservoir (*19*) and, on the other, east toward the Central Indian Ridge (CIR; Fig. 3A). This may explain the connection between La Réunion plume and the CIR, as suggested from geochemistry, and particularly the observed high-$^3He/^4He$ signature in enriched mid-ocean ridge basalt samples collected along the CIR axis (between 19°and 20°S) (*22*, *23*). This signature may therefore derive from the same lower-mantle plume source as that of La Réunion hot spot volcano, through multiple stages of alternating vertical and horizontal flow. On the other hand, the same asthenospheric pressure–driven flow extends westward toward the Mascareignes Basin, but the contamination does not seem to reach the Comores islands, which display a very different geochemical signature, with trace element geochemistry more akin to the East African rift signature (*24*, *25*).

DISCUSSION

The southeastern part of the Indian Ocean around La Réunion hot spot is located at the border of the African LLSVP. Our FWI-derived regional whole-mantle shear velocity model shows that, at least in this region, the LLSVP is not a broad continuous trunk structure extending high (1500 km) above the CMB as proposed by some authors (*5*, *11*) but rather consists of several distinct plumes rooted at the CMB and extending quasi-vertically over heights of ~2000 km. This suggests that the African LLSVP may be composed of a bundle of mantle plumes constrained by regions of subduction, as proposed in (*12*). These plumes encounter a region of resistance to vertical flow between 1000- and 660-km depth, the LSVPZ, where the flow spreads laterally, as is the case for other deep-mantle plumes, as previously imaged in other regions of the globe (*5*). This region has previously been proposed to be a region of stagnant plumes (*26*) and stagnant slabs (*27*). The presence of the ponding zone may be due to the negative Clapeyron slope of the 660-km discontinuity (*28*) combined with an increase in viscosity with a peak at around 1000-km depth (*29*, *30*), with possibly a zone of low viscosity between 660- and 1000-km depth (*30*). This depth range is, therefore, likely a zone of weakness that is the site of strong

Fig. 3. 3D rendering of the same subvolume, but highlighting the structure extended from mid-mantle to upper mantle (1700-to-200-km depth). 3D rendering of the same subvolume, but highlighting the structure extended from mid-mantle to upper mantle (1700-to-200-km depth). (A) The top surface is at 200-km depth and shows a low-velocity channel in the asthenosphere, extending between the CIR and Comores hotspot. (Band C) The top surface is at 300 and 400 km, respectively, and shows that the low-velocity channel in (A) is fed by a vertically oriented low-velocity conduit located not far from the projection of the La Réunion hot spot, itself arising from a horizontally extended zone of low velocities in the depth range of 1000 to 600 km. These topological relations may help explain the high–^{3}He/^{3}He isotopic ratio signature found along the CIR (22, 23).

horizontal shear (*21*) at the boundary between a vigorously convecting upper mantle and a more sluggish lower mantle (*31*). The lateral extent of the resolved ponding zones corresponding to La Réunion and Comores plumes as imaged here is on the order of ~2000 km (Fig. 1, D and E). Confirming other observations, for example, beneath the MacDonald, Canary, or Cape Verde hot spots (*5*), or the Yellowstone hot spot (*32*), our model suggests that the thinner plumes that arise from the LSVPZ toward hot spot volcanoes may be substantially offset from the location of the corresponding lower-mantle conduits. Our model also shows that another level of horizontal spreading and ponding may be present at shallower depths in the asthenosphere. Together, this may help explain trace element geochemistry over a wide radius away from the lowermost mantle source tapped by a plume rooted at the

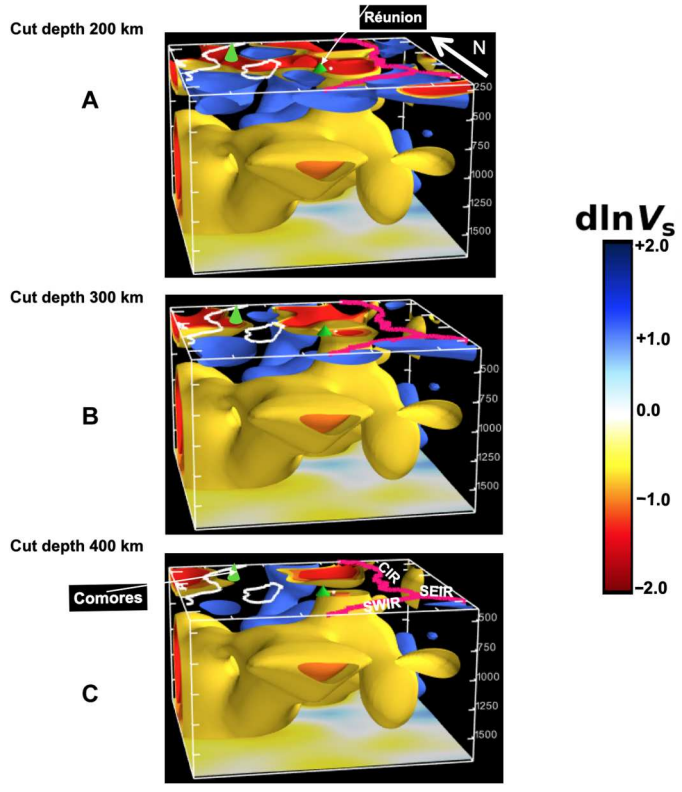

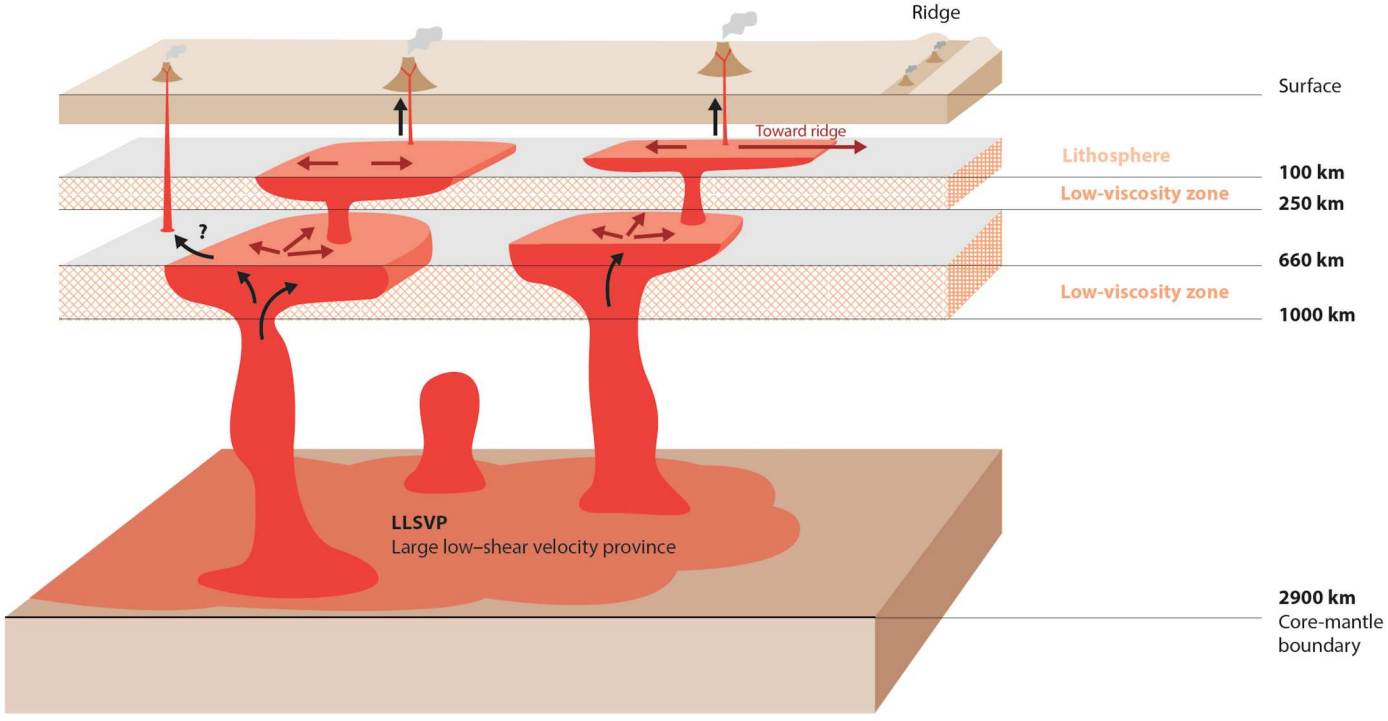

Fig. 4. Conceptual sketch illustrating the complexity of upwellings observed beneath hot spots in the Indian Ocean from the CMB up to the surface. The plumbing system consists of five stages: In the lower mantle, from the LLSVP up to ~1000 km, separate quasi-vertical fat plumes are observed, and in the upper mantle, from 660 km up to the asthenosphere, upwellings consist of thinner quasi-vertical plumes. Two wide zones of horizontal spreading and ponding (LSVPZ) are found, one in the depth range of ~1000 to 660 km and a second one in the asthenosphere at ~250 to 100 km (below the lithosphere), which does not have a clear lower-mantle root. In the final stage, the Indian Ocean hot spots of La Réunion and Comores as well as some parts of CIR are fed by the asthenospheric LSVPZ, also observed beneath the Mascareignes Basin (*19*). The question mark on the left denotes a potential connection between the lower-mantle LSVPZ and some other hot spots, such as the Marion hot spot as displayed in Fig. 1D. The surface location of a hot spot can be significantly offset with respect to its deep origin. The scale of the upper mantle is exaggerated. The complexity of whole mantle upwellings is reminiscent of the crustal volcano plumbing system with dykes and sills.

CMB. Our results suggest that the morphology of plume-like upwellings across the mantle and up to the asthenosphere consists of at least five stages that are just beginning to be resolved by mantle tomography: Regions of quasi-vertical flow respectively manifested in the lower mantle (from the CMB to 1000-km depth) by fat plumes and in the upper mantle (~660- to 250-km depth) by thinner plumes, separated by a zone of horizontal spreading in the extended transition zone, the LSVPZ. Another zone of horizontal spreading and ponding is the asthenosphere below the lithosphere, from which horizontal flow feeding mid-ocean ridges may originate (*33*). This is reminiscent of the volcanic plumbing system consisting of dykes and sills, as imaged in the Earth's crust, albeit here at a much larger, whole-mantle scale (Fig. 4). The deployment of temporary seismic stations around La Réunion island helped improve the resolution of the deep structure of La Réunion and Comores hot spots. A similar experiment should be performed in the southern Indian Ocean to improve the ray coverage around Marion, Kerguelen, and Crozet hot spots, and therefore their resolution at depth, to further our understanding of the deep plumbing system that brings upwelling flow from the CMB to the surface, within the footprint of the African LLSVP.

MATERIALS AND METHODS

The forward modeling in this study is based on spectral element method. Synthetic seismograms were computed on the CINES (Centre Informatique National de l'Enseignement Supérieur) platform, using the code CSEM (*34*). For the inverse step, the gradient and Hessian are obtained using nonlinear asymptotic coupling theory (*35*), and we lastly applied a Gauss-Newton optimization approach for each iteration (see the Supplementary Materials).

Supplementary Materials

This PDF file includes:

Section S1 to S3
Table S1
Figs. S1 to 12
References

REFERENCES AND NOTES

1. W. J. Morgan, Convection plumes in the lower mantle. *Nature* **230**, 42–43 (1971).
2. D. L. Anderson, Scoring hotspots: The plume and plate paradigms. *Geol. Soc. Am. Spec.* **388**, 31–54 (2005).
3. M. A. Richards, D. L. Jones, R. A. Duncan, D. J. DePaolo, A mantle plume initiation model for the Wrangellia flood basalt and other oceanic plateaus. *Science* **254**, 263–267 (1991).
4. E. J. Garnero, A. K. McNamara, S.-H. Shim, Continent-sized anomalous zones with low seismic velocity at the base of Earth's mantle. *Nat. Geosci.* **9**, 481–489 (2016).
5. S. W. French, B. Romanowicz, Broad plumes rooted at the base of the Earth's mantle beneath major hotspots. *Nature* **525**, 95–99 (2015).
6. V. Courtillot, G. Féraud, H. Maluski, D. Vandamme, M. G. Moreau, J. Besse, Deccan flood basalts and the Cretaceous/Tertiary boundary. *Nature* **333**, 843–846 (1988).
7. N. H. Sleep, Hotspots and mantle plumes: Some phenomenology. *J. Geophys. Res.* **95**, 6715–6736 (1990).
8. K. Farley, E. Neroda, Noble gases in the Earth's mantle. *Annu. Rev. Earth Planet. Sci.* **26**, 189–218 (1998).
9. M. Moreira, C. J. Allègre, Helium–neon systematics and the structure of the mantle. *Chem. Geol.* **147**, 53–59 (1998).
10. V. Courtillot, A. Davaille, J. Besse, J. Stock, Three distinct types of hotspots in the Earth's mantle. *Earth Planet. Sci. Lett.* **205**, 295–308 (2003).
11. M. Tsekhmistrenko, K. Sigloch, K. Hosseini, G. Barruol, A tree of Indo-African mantle plumes imaged by seismic tomography. *Nat. Geosci.* **14**, 612–619 (2021).
12. A. Davaille, B. Romanowicz, Deflating the LLSVPs: Bundles of mantle thermochemical plumes rather than thick stagnant piles. *Tectonics* **39**, e2020TC006265 (2020).
13. J.-P. Montagner, 3-Dimensional structure of the Indian Ocean inferred from long period surface waves. *Geophys. Res. Lett.* **13**, 315–318 (1986).
14. E. Debayle, J. Lévêque, Upper mantle heterogeneities in the Indian Ocean from waveform inversion. *Geophys. Res. Lett.* **24**, 245–248 (1997).
15. G. Barruol, K. Sigloch, Investigating La Réunion hot spot from crust to core. *Trans. Am. Geophys. Union* **94**, 205–207 (2013).
16. M. Wysession, D. Wiens, A. Nyblade, Investigation of sources of intraplate volcanism using PASSCAL broadband instruments in Madagascar, the Comores, and Mozambique. *Other/Seismic Network* (Washington University, 2011), vol. 10.
17. F. Tilmann, X. Yuan, G. Rümpker, E. Rindraharisaona, *Selasoma project, Madagascar 2012–2014. Deutsches Geoforschungszentrum GFZ. Seismic Network* (2012).
18. A. Mazzullo, E. Stutzmann, J. P. Montagner, S. Kiselev, S. Maurya, G. Barruol, K. Sigloch, Anisotropic tomography around La Réunion island from Rayleigh waves. *J. Geophys. Res.* **122**, 9132–9148 (2017).
19. G. Barruol, K. Sigloch, J. R. Scholz, A. Mazzullo, E. Stutzmann, J. P. Montagner, S. Kiselev, F. R. Fontaine, L. Michon, C. Deplus, J. Dyment, Large-scale flow of Indian Ocean asthenosphere driven by Réunion plume. *Nat. Geosci.* **12**, 1043–1049 (2019).
20. M. Wamba, J.-P. Montagner, B. Romanowicz, G. Barruol, Multi-mode waveform tomography of the Indian Ocean upper and mid-mantle around the Réunion hotspot. *J. Geophys. Res.* **126**, e2020JB021490 (2021).
21. J. A. Whitehead Jr., Instabilities of fluid conduits in a flowing earth are plates lubricated by the asthenosphere? *Geophys. J. Int.* **70**, 415–433 (1982).
22. J. Kim, S. J. Pak, J. W. Moon, S. M. Lee, J. Oh, F. M. Stuart, Mantle heterogeneity in the source region of mid-ocean ridge basalts along the northern Central Indian Ridge (8°S-17°S). *Geochem. Geophys. Geosystems* **18**, 1419–1434 (2017).
23. E. Füri, D. R. Hilton, B. J. Murton, C. Hémond, J. Dyment, J. M. D. Day, Helium isotope variations between Réunion Island and the Central Indian Ridge (17–21 S): New evidence for ridge–hot spot interaction (2011), vol. 116.
24. C. Class, S. L. Goldstein, M. Stute, M. D. Kurz, P. Schlosser, Grand Comore Island: A well-constrained "low ^{3}He/^{4}He" mantle plume. *Earth Planet. Sci. Lett.* **233**, 391–409 (2005).
25. T. O. Rooney, The Cenozoic magmatism of East Africa: Part V-magma sources and processes in the East African Rift. *Lithos* **360-361**, 105296 (2020).
26. L. Vinnik, S. Chevrot, J.-P. Montagner, Evidence for a stagnant plume in the transition zone? *Geophys. Res. Lett.* **24**, 1007–1010 (1997).
27. Y. Fukao, S. Widiyantoro, M. Obayashi, Stagnant slabs in the upper and lower mantle transition region. *Rev. Geophys.* **39**, 291–323 (2001).
28. C. R. Bina, G. Helffrich, Phase transition Clapeyron slopes and transition zone seismic discontinuity topography. *J. Geophys. Res.* **99**, 15853–15860 (1994).
29. J. Mitrovica, A. Forte, A new inference of mantle viscosity based upon joint inversion of convection and glacial isostatic adjustment data. *Earth Planet. Sci. Lett.* **225**, 177–189 (2004).
30. M. L. Rudolph, V. Lekić, C. Lithgow-Bertelloni, Viscosity jump in Earth's mid-mantle. *Science* **350**, 1349–1352 (2015).
31. K. Yuan, B. Romanowicz, Seismic evidence for partial melting at the root of major hot spot plumes. *Science* **357**, 393–397 (2017).
32. P. L. Nelson, S. P. Grand, Lower-mantle plume beneath the Yellowstone hotspot revealed by core waves. *Nat. Geosci.* **11**, 280–284 (2018).
33. J. Morgan, J. Hasenclever, C. Shi, New observational and experimental evidence for a plume-fed asthenosphere boundary layer in mantle convection. *Earth Planet. Sci. Lett.* **366**, 99–111 (2013).
34. Y. Capdeville, E. Chaljub, J. P. Montagner, Coupling the spectral element method with a modal solution for elastic wave propagation in global Earth models. *Geophys. J. Int.* **152**, 34–67 (2003).
35. X.-D. Li, B. Romanowicz, Global mantle shear velocity model developed using nonlinear asymptotic coupling theory. *J. Geophys. Res.* **101**, 22245–22272 (1996).
36. S. Maurya, J. P. Montagner, M. R. Kumar, E. Stutzmann, S. Kiselev, G. Burgos, N. P. Rao, D. Srinagesh, Imaging the lithospheric structure beneath the Indian continent. *J. Geophys. Res.* **121**, 7450–7468 (2016).
37. S. French, B. Romanowicz, Whole-mantle radially anisotropic shear velocity structure from spectral-element waveform tomography. *Geophys. J. Int.* **199**, 1303–1327 (2014).
38. K. Hosseini, K. J. Matthews, K. Sigloch, G. E. Shephard, M. Domeier, M. Tsekhmistrenko, SubMachine: Web-based tools for exploring seismic tomography and other models of Earth's deep interior. *Geochem. Geophys. Geosystems* **19**, 1464–1483 (2018).
39. D. Komatitsch, J. Tromp, Introduction to the spectral element method for three-dimensional seismic wave propagation. *Geophys. J. Int.* **139**, 806–822 (1999).

40. B. Kustowski, G. Ekström, A. Dziewoński, Anisotropic shear-wave velocity structure of the Earth's mantle: A global model. *J. Geophys. Res.* **113**, B06306 (2008).
41. W. Lei, Y. Ruan, E. Bozdağ, D. Peter, M. Lefebvre, D. Komatitsch, J. Tromp, J. Hill, N. Podhorszki, D. Pugmire, Global adjoint tomography model GLAD-M25. *Geophys. J. Int.* **223**, 1–21 (2020).
42. X.-D. Li, B. Romanowicz, Comparison of global waveform inversions with and without considering cross-branch modal coupling. *Geophys. J. Int.* **121**, 695–709 (1995).
43. J. Ritsema, A. Deuss, H. Van Heijst, J. Woodhouse, S40RTS: A degree-40 shear velocity model for the mantle from new Rayleigh wave dispersion, teleseismic traveltime and normal-mode splitting function measurements. *Geophys. J. Int.* **184**, 1223–1236 (2011).
44. A. Tarantola, B. Valette, Generalized nonlinear inverse problems solved using the least squares criterion. *Rev. Geophys. Phys.* **20**, 219–232 (1982).

Acknowledgments: We thank F. J. Simons and J. Irving for valuable discussions and A. Schroeder for Fig. 4 improvement. We also thank S. Maurya who provided some Indian processed broadband data (*36*) and the anonymous reviewers for valuable suggestions that considerably improve the manuscript. We thank Tiger (Princeton Supercomputer) & CINES (Centre Informatique National de l'Enseignement Supérieur) for providing computational resources. **Funding:** This work was supported by a grant from Princeton University (Presidential Fellowship) and Collège de France. J.-P.M. acknowledges support from the IUF (Institut Universitaire de France), and B.R. acknowledges support from NSF grant EAR 1758198. **Author contributions:** B.R. and J.-P.M. led the design of the project and contributed to the analysis and interpretation of the results. B.R. provided guidance on the waveform processing and inversion methodology and drafted the sketch in Fig. 4. M.D.W. collected the waveform data and performed the model construction. All authors contributed to writing the manuscript. **Competing interests:** The authors declare that they have no competing interests. **Data and materials availability:** All data needed to evaluate the conclusions in the paper are present in the paper and/or the Supplementary Materials. Additional data related to this paper can be downloaded from the links below. The RHUM-RUM data (https://doi.org/10.15778/RESIF.YV2011) were transferred into the International Federation of Digital Seismograph Networks (FDSN) with the code YV. Some of the data were collected from Incorporated Research Institutions for Seismology (IRIS). We also used data from the permanent networks of GEOSCOPE (https://doi.org/10.18715/GEOSCOPE.G) and GSN (https://doi.org/10.7914/SN/IU) and seismic data from the temporary experiments around Madagascar, Selasoma (http://doi.org/10.14470/MR7567431421).

Submitted 11 August 2022
Accepted 28 December 2022
Published 25 January 2023
10.1126/sciadv.ade3723

ScienceAdvances

Imaging deep-mantle plumbing beneath La Réunion and Comores hot spots: Vertical plume conduits and horizontal ponding zones

Mathurin Dongmo Wamba, Jean-Paul Montagner, and Barbara Romanowicz

Sci. Adv., **9** (4), eade3723.
DOI: 10.1126/sciadv.ade3723

Science Advances (ISSN) is published by the American Association for the Advancement of Science. 1200 New York Avenue NW, Washington, DC 20005. The title *Science Advances* is a registered trademark of AAAS.